

Propulsive Aerodynamics of an Advanced Nozzle/Forward Swept Wing Aircraft Configuration

Douglas L. Bowers*

USAF Wright Aeronautical Laboratories, Wright-Patterson Air Force Base, Ohio

Nonaxisymmetric exhaust nozzles can offer advanced aircraft configurations improved performance through the propulsive-aerodynamic interaction of the jet exhaust and the wing flowfield. An experimental investigation of this interaction was conducted at Mach numbers from 0.3 to 0.9 on a half-span wing-body configuration with vectoring (0, 15, 30 deg) nonaxisymmetric exhaust nozzles incorporated into the trailing edge of a forward swept wing. Results indicate that at all Mach numbers, the aerodynamic lift and drag coefficients increase while the pitching moment coefficient becomes more negative with increasing nozzle vectoring and nozzle flow. Thrust vectoring improves the aircraft drag polar especially at higher angles of attack.

Nomenclature

A	= aspect ratio
$b/2$	= model half span, in.
C_D	= drag coefficient (D/qS)
C_{D-T}	= drag minus thrust coefficient [$(D-T)/qS$]
C_L	= lift coefficient (L/qS)
C_M	= pitching moment coefficient (moment/ $qS\bar{c}$)
C_p	= pressure coefficient [$(P-P_\infty)/q$]
C_T	= thrust coefficient (T/qS)
\bar{c}	= mean aerodynamic chord, in.
D	= drag, lb
L	= lift, lb
M	= Mach number
NPR	= nozzle pressure ratio (P_{T_n}/P_∞)
P	= local static pressure, psi
P_{T_n}	= total pressure at nozzle throat, psi
P_∞	= freestream static pressure, psi
S	= reference area, 27.528 in. ² (approximate trapezoidal half-span wing area)
T	= thrust, lb
q	= dynamic pressure, psi
X_c	= distance from wing leading edge referenced to chord length at wing pressure orifices
$Y_{b/2}$	= distance from wing root referenced to wing semi-span
α	= angle of attack, deg

Introduction

THE nonaxisymmetric exhaust nozzle is a maturing technology that shows promise for utilization on advanced aircraft. Benefits identified for nonaxisymmetric nozzles include 1) increased lift due to the induced aerodynamics attributed to the exhaust nozzle flow near a lifting surface; 2) increased instantaneous lift due to a vectored exhaust jet; 3) improved deceleration during flight and on landing when a thrust reverser is incorporated; and 4) reduced aircraft observables, i.e., radar cross section and infrared signature. These benefits are not only related to unique nozzle geometry but also to the interaction of the exhaust nozzle flow and the wing flowfield. Previous studies¹⁻⁸ have indicated large favorable interactions can occur when the nozzle exit is geometrically located at or near the wing trailing

edge. As shown in Fig. 1, at 0.9 Mach number, the jet induced lift from these interactions can be as large as the direct jet lift. In that case, the aircraft wing aerodynamics and the propulsion system performance can not be separated because the propulsion system flow influences the aircraft lift, drag, and pitching moment. It is these propulsive-aerodynamic interactions that are addressed in this paper.

The forward swept wing is another emerging technology for advanced tactical aircraft. Potential benefits identified for this technology include 1) improved low speed aircraft handling characteristics; 2) increased resistance to spin/departure; 3) reduced aircraft stall speed; and 4) improved lift-to-drag ratio during aircraft maneuvering. The nonaxisymmetric exhaust nozzle and forward swept wing can both be incorporated on an aircraft to take advantage of the potential benefits of these technologies. For example, the good low speed aircraft handling characteristics with the forward swept wing and the improved instantaneous maneuvering attributed to a vectored nonaxisymmetric exhaust nozzle can be combined to produce an aircraft configuration with superior performance across the entire mission spectrum. A representative advanced aircraft configuration of this type is shown in Fig. 2.

While a forward swept wing aircraft design was used, the main focus of this program was the integrated nonaxisymmetric exhaust nozzle. The purpose of this investigation was to explore the interactive aerodynamics of a wing/body configuration with a vectored high aspect ratio nonaxisymmetric exhaust nozzle.

Description of the Aeropropulsion Model

The wind tunnel model utilized in this effort was available equipment at the Air Force Wright Aeronautical Laboratories Flight Dynamics Laboratory Trisonic Gasdynamics Facility (TGF). The half-span model, shown in Fig. 3, was a wing/body/canard configuration with interchangeable exhaust nozzles incorporated into the wing trailing edge near the wing root. The primary instrumentation was a five-component force balance which measured the forces on the entire model from which lift, drag, and pitching moment coefficients were determined.

The forward swept wing planform had a leading edge sweep of -15 deg and a trailing edge sweep of -42 deg. The wing airfoil varied from a NACA 64A006 at the wing root to a NACA 64A003 at the wing tip, though the wing profile is modified in the wing root area to accommodate the exhaust nozzle as shown in Fig. 3. The wing was instrumented with limited upper surface static pressure orifices near the area of influence for the exhaust nozzle flow.

A canard, located on the fuselage forward and above the wing, was also tested. The canard planform was ap-

Presented as Paper 80-1158 at the AIAA/SAE/ASME 16th Joint Propulsion Conference, Hartford, Conn., June 30-July 2, 1980; submitted Aug. 22, 1980; revision received Jan. 27, 1981. This paper is declared a work of the U.S. Government and therefore is in the public domain.

*Aerospace Engineer, Flight Dynamics Laboratory, Member AIAA.

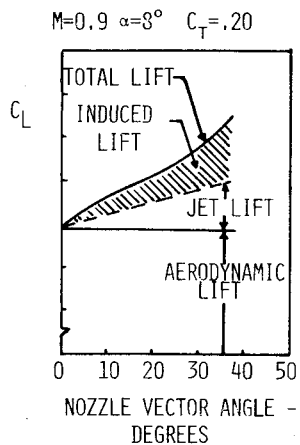


Fig. 1 Components of lift due to thrust vectoring.

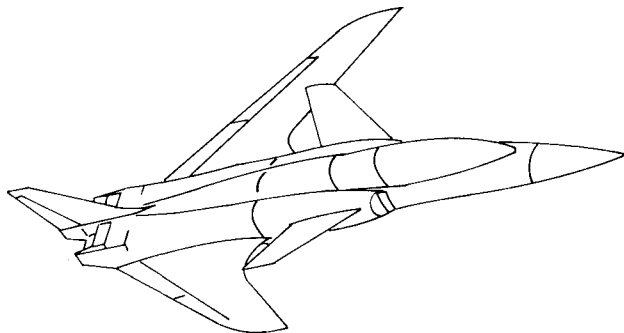


Fig. 2 Advanced aircraft configuration.

proximately 20% of the wing planform area and had a NACA airfoil 64A204.

To nonaxisymmetric exhaust nozzles were convergent type with a width approximately 20% of the wing span from the wing body junction. High-pressure cold air was used to simulate the jet exhaust. Vectoring of the convergent exhaust nozzles to the 15- and 30-deg geometric vector angles was accomplished by turning the last 5% of the nozzle surfaces into the freestream flow (see Fig. 3). The aspect ratio of these nonaxisymmetric exhaust nozzles (defined as the ratio of the exhaust nozzle width to height at the nozzle throat) was approximately 11.0.

To separate the exhaust nozzle thrust from the total configuration forces, the exhaust nozzle, the body, and a small portion of the wing surface forward of the nozzle (shown cross-hatched in Fig. 3) were tested at static conditions at the scheduled nozzle pressure ratios with the wind tunnel pumped down to the static pressure corresponding to the wind-on test Mach number conditions. The force balance measured the static components of normal and axial forces as well as pitching moment due to the thrust for the vectored nozzles. These thrust force components were then subtracted from the wind-on full wing/body configuration data to obtain the thrust-removed aerodynamic components.

Facility Description and Test Parameters

The Trisonic Gasdynamics Facility, located at Wright-Patterson Air Force Base, is a closed-circuit variable-density continuous-flow wind tunnel with an operating Mach number range of 0.23-3.00. Two test sections were utilized for this effort. For the subsonic Mach numbers from 0.3 to 0.7, the solid wall 2×2 ft test section was used with the half-span model mounted directly to a wall plate. A transonic test section, 15×15 in.² with slotted sidewalls top and bottom, was utilized for a portion of the 0.7 and all of the 0.8 and 0.9 Mach number data.

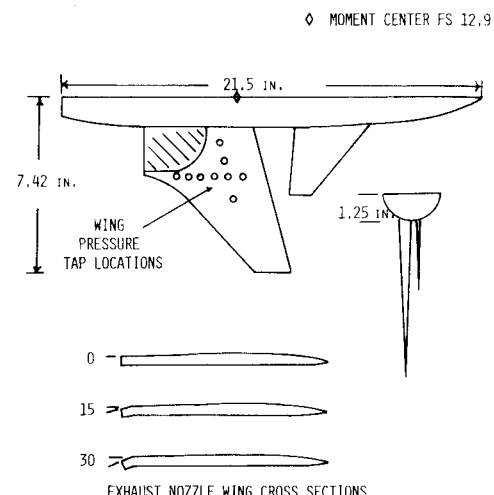
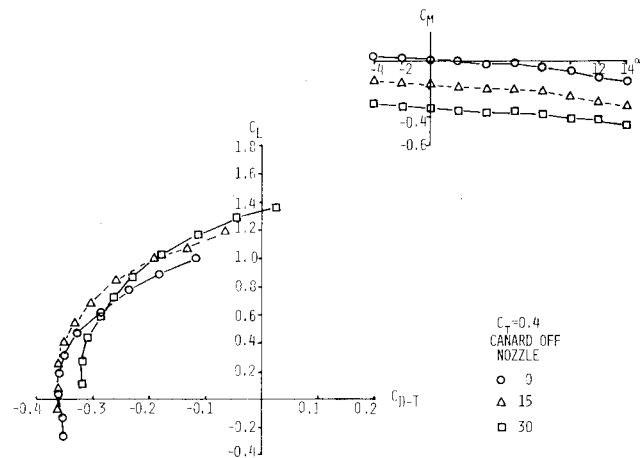


Fig. 3 Half-span test model.

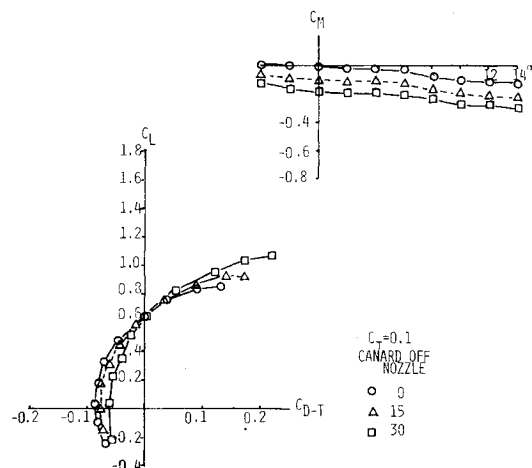
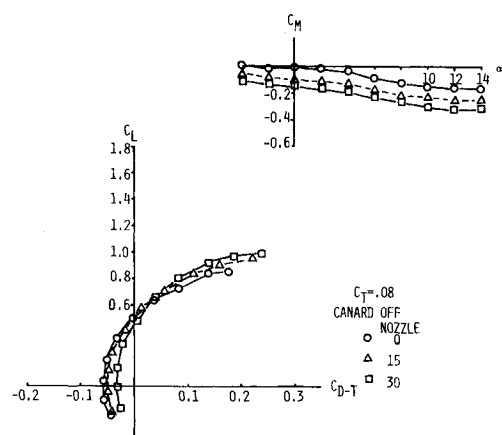
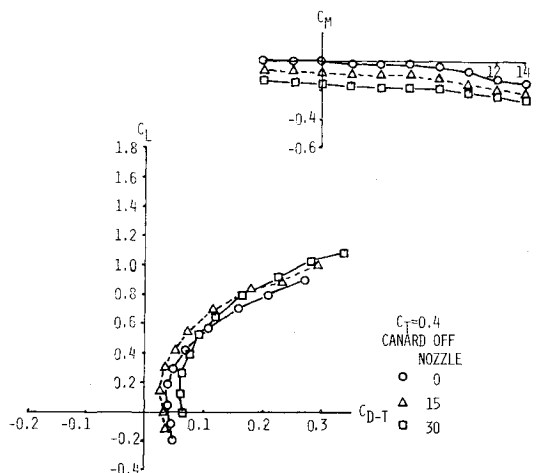
Fig. 4 Powered polar, $M = 0.3$, $NPR = 3$.

Nominal test parameters were 0.3-0.9 Mach numbers, angles of attack from -4 to 15 deg, and a unit Reynolds number of 2.0×10^6 /ft.

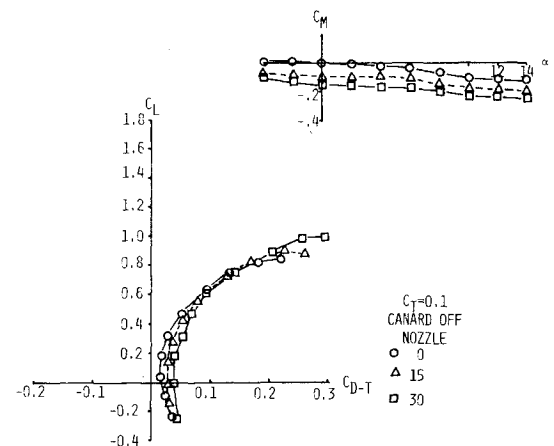
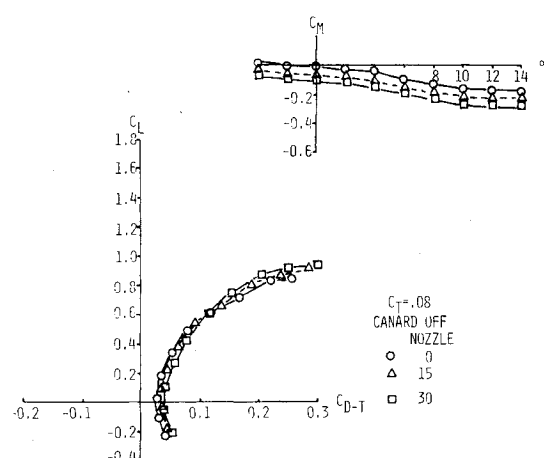
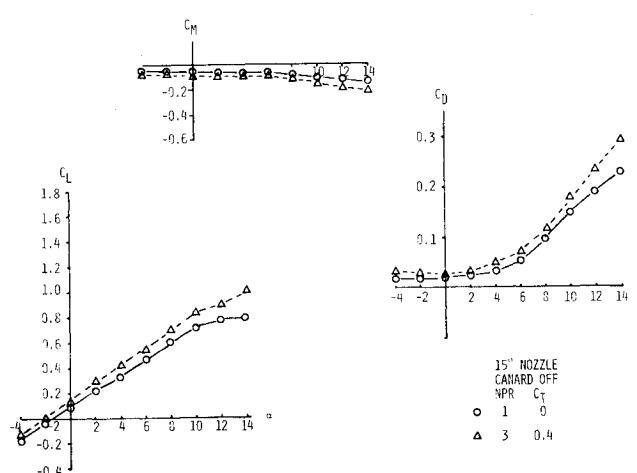
Aerodynamic Interactions Due to Thrust Vectoring

A combination of the aerodynamic and propulsion forces of an aircraft configuration are included in the powered drag polar or total performance polar of that vehicle. The powered polars for this configuration are shown in Figs. 4-6 at Mach numbers of 0.3, 0.6, and 0.9. These conditions will be used as representative of the other Mach number data obtained. For all the powered polars, the vectored exhaust nozzle polar crosses over the nonvectored exhaust nozzle polar. A portion of each powered polar can be utilized to form an optimum powered polar which is better than any other polar at a fixed thrust vector angle.

The powered polars indicate a favorable influence for a vectorable nonaxisymmetric nozzle with the forward swept wing, especially at high angles of attack or high lift coefficients and at the lower Mach numbers 0.3 and 0.6. While this is untrimmed data, the improvement in the drag polar is not expected to be completely negated by trim considerations. These improvements can be attributed to three sources: 1) the direct jet lift, 2) the induced aerodynamics of the exhaust flow, and 3) the "flap" or camber effect of the turned down nozzle surface. The last two components will be analyzed to determine the relative contributions of each to the vectored nozzle/wing interaction.

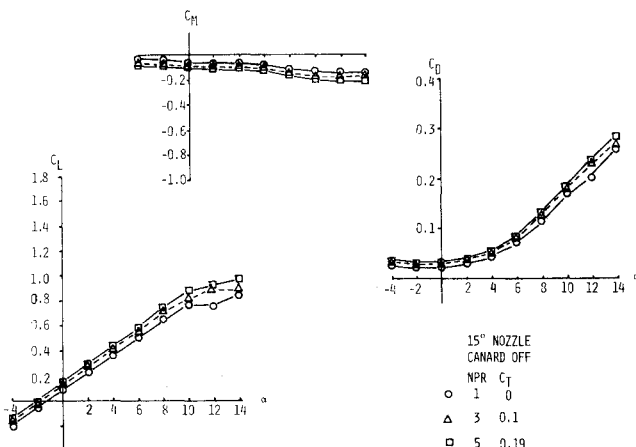
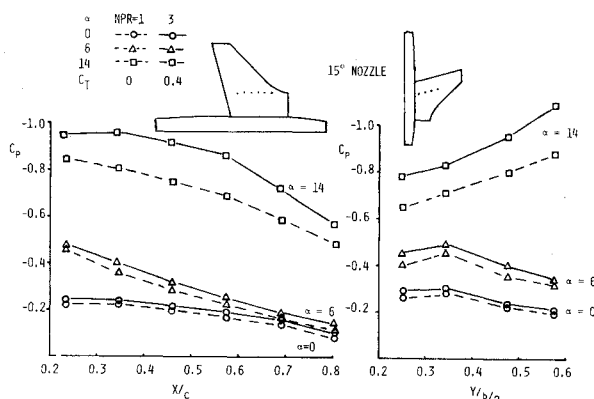
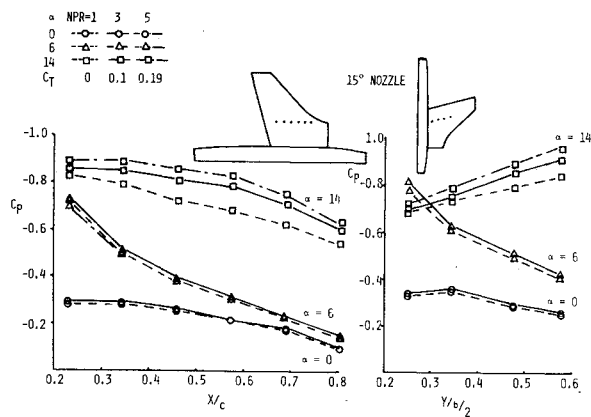
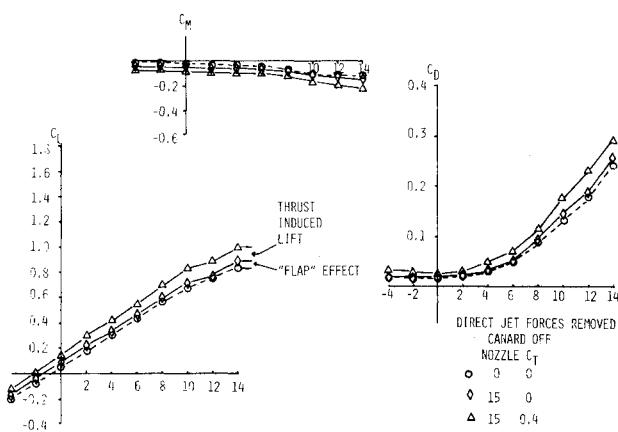
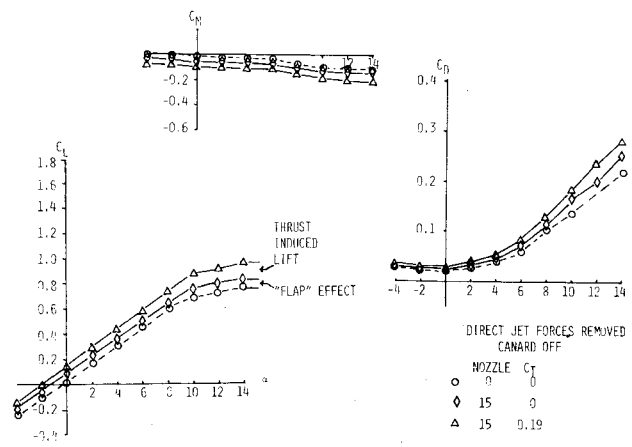
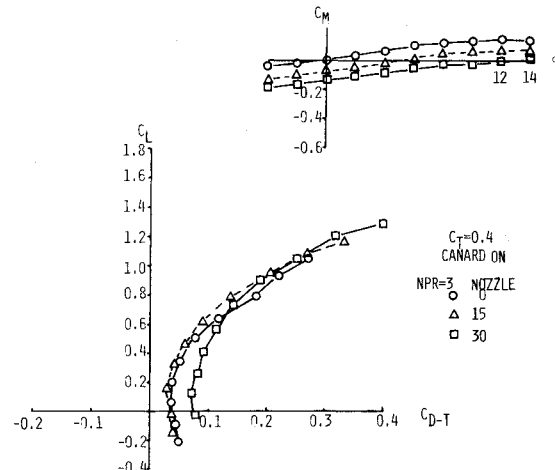
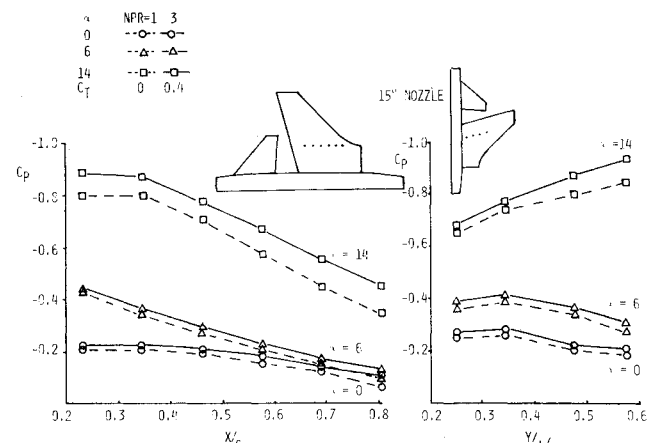
Fig. 5 Powered polar, $M = 0.6$, $NPR = 3$.Fig. 6 Powered polar, $M = 0.9$, $NPR = 5$.Fig. 7 Thrust removed drag polar, $M = 0.3$, $NPR = 3$.

If the direct jet is removed from the lift, drag, and pitching moment coefficients, the induced aerodynamic effects and the flap effect remain. Thrust-removed drag polars for 0.3, 0.6, and 0.9 Mach numbers are shown in Figs. 7-9. A benefit for thrust vectoring at high angles of attack is still evident for all Mach numbers though the increment at 0.9 Mach number is small. Both vectored nozzle polars cross over the unvectored polar and the 30-deg polar crosses over the 15-deg polar as the angle of attack is increased. The large favorable shift in the 15-deg drag polar is thought to be due to a reduction of separated flow in the wing root area with the jet on and deflected. While the potential for flow improvement in wing

Fig. 8 Thrust removed drag polar, $M = 0.6$, $NPR = 3$.Fig. 9 Thrust removed drag polar, $M = 0.9$, $NPR = 5$.Fig. 10 Induced aerodynamic components, $M = 0.3$.

root area is also present for the 30-deg nozzle, the increased drag from the flap effect of the turned down 30-deg nozzle surface is greater than the 15-deg nozzle and therefore a benefit in the jet off polar is not present. A benefit is also apparent in the powered polar at low angles of attack (Fig. 4) with the 15-deg nozzle.

The induced (thrust-removed) aerodynamic contributions to lift, drag, and pitching moment coefficient for Mach numbers of 0.3 and 0.6 are shown in Figs. 10 and 11. The induced aerodynamics are a result of the exhaust nozzle flow changing the pressure distribution around the wing surface. At constant angle of attack, the influence of the jet produces

Fig. 11 Induced aerodynamic components, $M = 0.6$.Fig. 12 Wing pressure coefficients, $M = 0.3$, canard off.Fig. 13 Wing pressure coefficients, $M = 0.6$, canard off.Fig. 14 Contribution of flap effect, $M = 0.3$.Fig. 15 Contribution of flap effect, $M = 0.6$.Fig. 16 Thrust removed drag polar, $M = 0.3$.Fig. 17 Wing pressure coefficients, $M = 0.3$, canard on.

increased lift, increased drag, and a change in pitching moment relative to the nozzle pressure ratio. The penalties for induced lift from the nozzle vectoring include induced drag and pitching moment change. These changes in aerodynamic coefficients are substantiated by the change in upper surface wing pressures ahead of the exhaust nozzle, as indicated in Figs. 12 and 13. For both 0.3 and 0.6 Mach number, the increase in nozzle pressure ratio decreased the upper surface wing pressures corresponding to the changes in induced aerodynamic coefficients shown in the previous figures.

The final contribution to the vectoring powered polar changes is due to the flap effect, i.e. the last 5% of the nozzle/wing surface that is deflected into the freestream and

behaves like an aerodynamic control surface. That flap effect can be seen in Figs. 14 and 15 for 0.3 and 0.6 Mach number. In both cases, this effect is small though the 0.6 Mach number data shows a proportionally larger flap contribution to the total propulsive-aerodynamic interaction at the higher dynamic freestream pressure.

To trim out nozzle vectoring moments, advanced aircraft designs utilize relaxed static stability and canards. For selected conditions in this test, a fixed fuselage mounted canard was investigated. The thrust-removed drag polar and pitching moment with the canard on are shown in Fig. 16. With the canard on at low angles of attack, deflecting the nozzle 15 deg results in a better drag polar than when the nozzle is not deflected. Utilizing the 30-deg nozzle gives a better drag polar at the higher angles of attack. These improvements are similar to the canard off results. As shown in Fig. 17, the canard downwash tends to suppress the wing pressures, though the relative level of pressure coefficient change due to thrust induced effects and therefore the nozzle/wing interaction does not appear to be affected.

Conclusions

Based on the data generated and analyzed in this effort, the following conclusions can be made.

1) Powered polars, untrimmed, indicate benefits for thrust vectoring especially at high lift coefficients for all Mach numbers presented ($M = 0.3-0.9$).

2) Changes in total lift, drag, and pitching moment coefficients are due to direct jet lift, jet induced aerodynamics, and the flap effect of the exhaust nozzle surface turned into the freestream flow. As Mach number increases, the contribution of the induced aerodynamic effects decreases and the contribution of the exhaust nozzle flap effect increases. In other words, the interactions of the jet exhaust flow and the wing flowfield decrease as Mach numbers increase.

3) The thrust induced effects increase as the nozzle thrust coefficient increases.

4) The change in upper surface wing pressure coefficients substantiate the data trends for all exhaust nozzles and test conditions.

5) The incorporation of a vectorable nonaxisymmetric nozzle with this forward swept wing aircraft configuration resulted in an improved powered polar over an unvectored nozzle configuration.

References

¹Hiley, P.E., Wallace, H.W., and Booz, D.E., "Study of NonAxisymmetric Nozzles Installed in Advanced Fighter Aircraft," *Journal of Aircraft*, Vol. 13, Dec. 1976, pp. 1000-1006.

²Yoshihara, H., Benepe, D.B., and Whitten, P.D., "Transonic Performance of Jet Flaps on an Advanced Fighter Configuration," AFFDL-TR-73-97, July 1973.

³Bradley, R.C., Jeffries, R.R., and Capone, F.J., "A Vectored Engine-Over-Wing Propulsive-Lift Concept," AIAA Paper 76-917, AIAA Aircraft Systems and Technology Meeting, Dallas, Texas, Sept. 1976.

⁴Reubush, D.E., "An Investigation of Induced Drag Reduction Through Over-The-Wing Blowing," AIAA Paper 77-884, AIAA/SAE 13th Propulsion Conference, Orlando, Fla., July 1977.

⁵Capone, F.J., "Supercirculation Effects Induced by Vectoring a Partial-Span Rectangular Jet," AIAA Paper 74-971, AIAA 6th Aircraft Design, Flight Test, and Operations Meeting, Los Angeles, Calif., Aug. 1974.

⁶Capone, F.J., "A Summary of Experimental Research on Propulsive-Lift Concepts in the Langley 16-Foot Transonic Tunnel," AIAA Paper 75-1315, AIAA/SAE 11th Propulsion Conference, Anaheim, Calif., Sept. 1975.

⁷Buchan, F., "An Investigation of a Two-Dimensional Vectored Nozzle From a Wing Training Edge," Air Force Institute of Technology, AFIT/GAE/AA/77D-3, Dec. 1977.

⁸Bowers, D.L. and Buchan, F., "An Investigation of the Induced Aerodynamic Effects of a Vectored Non-Axisymmetric Exhaust Nozzle," AIAA Paper 78-1082, AIAA 14th Joint Propulsion Conference, Las Vegas, Nev., July 1978.

From the AIAA Progress in Astronautics and Aeronautics Series

ALTERNATIVE HYDROCARBON FUELS: COMBUSTION AND CHEMICAL KINETICS—v. 62

A Project SQUID Workshop

Edited by Craig T. Bowman, Stanford University
and Jørgen Birkeland, Department of Energy

The current generation of internal combustion engines is the result of an extended period of simultaneous evolution of engines and fuels. During this period, the engine designer was relatively free to specify fuel properties to meet engine performance requirements, and the petroleum industry responded by producing fuels with the desired specifications. However, today's rising cost of petroleum, coupled with the realization that petroleum supplies will not be able to meet the long-term demand, has stimulated an interest in alternative liquid fuels, particularly those that can be derived from coal. A wide variety of liquid fuels can be produced from coal, and from other hydrocarbon and carbohydrate sources as well, ranging from methanol to high molecular weight, low volatility oils. This volume is based on a set of original papers delivered at a special workshop called by the Department of Energy and the Department of Defense for the purpose of discussing the problems of switching to fuels producible from such nonpetroleum sources for use in automotive engines, aircraft gas turbines, and stationary power plants. The authors were asked also to indicate how research in the areas of combustion, fuel chemistry, and chemical kinetics can be directed toward achieving a timely transition to such fuels, should it become necessary. Research scientists in those fields, as well as development engineers concerned with engines and power plants, will find this volume a useful up-to-date analysis of the changing fuels picture.

463 pp., 6 x 9 illus., \$20.00 Mem., \$35.00 List

TO ORDER WRITE: Publications Dept., AIAA, 1290 Avenue of the Americas, New York, N.Y. 10019